An Iterative Extended Boundary Condition Method for Solving the Absorption Characteristics of Lossy Dielectric Objects of Large Aspect Ratios

A. LAKHTAKIA, STUDENT MEMBER, IEEE, M. F. ISKANDER, MEMBER, IEEE, AND C. H. DURNEY, SENIOR MEMBER, IEEE

Abstract—**The recently developed iterative extended boundary condition method (IEBCM) has been used to compute the internal fields induced in homogeneous, axisymmetric, lossy dielectric objects of large aspect ratios when exposed to incident planewave radiation. Calculations were made for both the E- and k-polarization cases. The computed results for a prolate spheroidal model of an average man are found to be accurate for frequencies up to 300 MHz, while the use of the popular EBCM [1] was found to be essentially restricted to frequencies less than 70 MHz for these models and exposure conditions.**

The applicability of the IEBCM to composite bodies has also been examined by studying the irradiation of a capped cylindrical object. This composite object was first partitioned into several overlapping spherical subregions, and, alternatively, into two spherical subregions overlapping with a central cylindrical subregion. Spherical harmonics were used to represent the internal fields in the spherical subregions, while cylindrical expansions were utilized in the cylindrical subregions. It is shown that the second partitioning scheme is more computationally efficient and thereby suggests that the basis functions used to represent the subregional fields should be compatible with the subregional geometry. The new IEBCM, therefore, is a very valuable procedure which provides the opportunity of using the mixed basis functions in the solution.

I. INTRODUCTION

AN ONGOING research project at the University of Utah has been the theoretical quantitation of the energy deposition in biological objects exposed to nonionizing radiation at the lower microwave frequencies. In this context, some of the first studies carried out involved the characterization of the power absorption in homogeneous, lossy dielectric, prolate spheroidal models of humans and animals exposed to plane waves and various near-field sources [1]–[7]. In all of these references, the electromagnetic (EM) boundary value problem, associated with the scattering and the absorption of the EM waves by the lossy dielectric spheroids, was solved using the popular extended boundary condition method (EBCM) initially formulated by Waterman [8], [9] and extensively used by others in several alternative formulations [10]–[12] for various other applications [13]–[15]. We noticed, however, that the EBCM fails to yield convergent internal field distributions in lossy dielectric objects in the resonance and the post-resonance frequency ranges for objects of large aspect ratios. By the term "aspect ratio" we mean the ratio of the largest to the smallest linear dimensions of the object. This deficiency in the EBCM is due to the use of the ill-conditioned system of equations that result from taking a large number of terms in order to force a single vector spherical harmonic expansion [16] to fit a nonspherical object [17].

In order to overcome the convergence-related stability problems in the EBCM, we have proposed and examined a new iterative technique elsewhere [18], [19]. This technique, called the iterative EBCM (IEBCM), is an iterative procedure which has two main features: a) it requires an initial estimate of the tangential fields on the object surface, and b) the fields induced inside the object are represented by several overlapping subregional expansions. Since the biological objects are characterized by large, complex relative permittivities, the initial estimate required by a) may be obtained by replacing the dielectric object by a perfectly conducting one of the same shape and size, and then solving for the current densities on the surface of the substitute object as has been suggested by others previously [20], [21]. The specific use of the several subregional expansions to represent the internal fields as indicated in b), on the other hand, allows us to obtain continuous and convergent internal field values throughout the internal volume by partitioning the object volume into a number of overlapping subregions, in each of which a separate internal field representation is assumed. In addition, these subregional expansions are linked to each other by being explicitly matched in the appropriate overlapping zones. Since all the subregional internal field expansions are simultaneously solved for in any given iterative step of the IEBCM, continuous and convergent internal field distributions are assured.

In this paper we present the application of the IEBCM to calculate the power absorption in biological models exposed to incident plane-wave radiation in the resonance and the post-resonance frequency ranges. Specifically, we compute the average specific absorption rate (SAR) [2] in a prolate spheroidal model of an average man exposed to incident E- and k-polarized plane waves [2]. In addition, we also examine the application of the IEBCM to solving

Manuscript received November 5, 1982; revised April 12, 1983.

The authors are with the Department of Electrical Engineering, University of Utah, Salt Lake City, UT 84112

0018-9480/83/0800-0640$01.00 ©1983 IEEE

for composite bodies, for which purpose the internal fields induced inside a capped cylindrical model of an average man were computed. The interior volume of the capped cylindrical object was first divided into several overlapping spherical subregions and the fields in each of which were expressed in terms of the vector spherical harmonics. The same volume was alternatively partitioned into a finite cylindrical subregion in the middle section and two spherical subregions to account for the hemispherical end caps. Spherical expansions were used in the two spherical subregions and a cylindrical expansion was utilized for the cylindrical subregion. Numerical results illustrating the importance and the limitations of using different basis functions are presented. In particular, we shall present results to compare the computational efficiency incurred in the use of the different basis functions to represent the various subregional fields induced in the interior volume of this object.

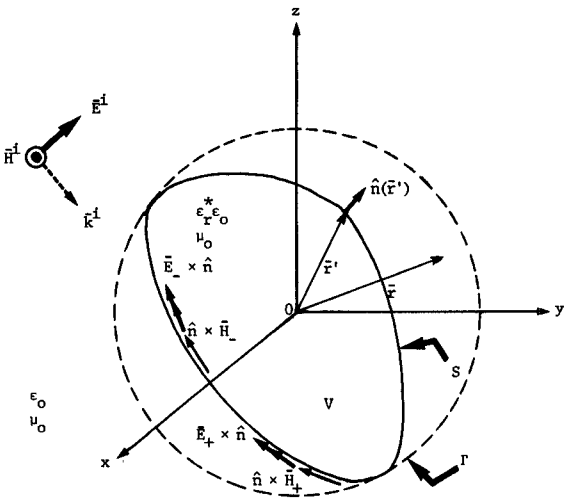

Fig. 1. Geometry associated with the IEBCM formulation. The various electromagnetic quantities involved are also represented.

II. Formulation

The IEBCM formulation has been discussed in an earlier publication by our group [19], but for the sake of completeness, a summary of the procedure is presented here. Consider a biological model having a volume V bounded by a closed smooth surface S, which lies totally inside a minimum sphere Γ and is characterized by a complex relative permittivity ϵ_r^*, as shown in Fig. 1. For a given incident EM field $\{\bar{E}^i(\bar{r}), \bar{H}^i(\bar{r})\}$ at any point $\bar{r}$ specified with respect to an origin O located suitably inside the model, it is desired to compute the fields induced inside the lossy dielectric volume V. By using the equivalence principle, the fields induced inside the object are replaced by equivalent electric and magnetic surface current densities. Therefore, upon applying the boundary conditions on the surface S and equating the total fields in the interior of the model to zero, the following integral equation for the external electric and magnetic fields, $\bar{E}_+$ and $\bar{H}_+$, on the surface S is obtained [22]:

$$-\bar{E}^i(\bar{r}) = \nabla \times \int_S \left[\hat{n}(\bar{r}') \times \bar{E}_+(\bar{r}')\right] \cdot \bar{G}(k\bar{r}|k\bar{r}')\, ds'$$

$$-\nabla \times \nabla \times \int_S \frac{1}{j\omega\epsilon_o} \left[\hat{n}(\bar{r}') \times \bar{H}_+(\bar{r}')\right] \cdot \bar{G}(k\bar{r}|k\bar{r}')\, ds' \quad (1)$$

where $k = \omega\sqrt{\mu_0\epsilon_0}$ is the free-space wavenumber, $\hat{n}$ is a unit outward normal to S, and $\bar{G}(k\bar{r}|k\bar{r}')$ is the free-space transverse Green's dyadic function discussed in [23].

Equation (1) is the basic equation involved in EBCM [8], [22], and it is modified into a form suitable for the lth ($l \geq 0$) IEBCM iteration as follows [18], [19]:

$$\left\{\bar{E}^i(\bar{r}) + \Delta \times \int_S \left[\hat{n}(\bar{r}') \times \bar{E}_{int}^{(l-1)}(\bar{r}')\right] \cdot \bar{G}(k\bar{r}|k\bar{r}')\, ds' \right.$$

$$\left. -\nabla \times \nabla \times \int_S \frac{1}{j\omega\epsilon_o} \left[\hat{n}(\bar{r}') \times \bar{H}_{int}^{(l-1)}(\bar{r}')\right] \cdot \bar{G}(k\bar{r}|k\bar{r}')\, ds' \right\}$$

$$= \nabla \times \nabla \times \int_S \frac{1}{j\omega\epsilon_0} \left[\hat{n}(\bar{r}') \times \Delta\bar{H}_+^{(l)}(\bar{r}')\right] \cdot \bar{G}(k\bar{r}|k\bar{r}')\, ds'. \quad (2)$$

In (2), the only unknown quantity is the incremental electric surface current density $\hat{n} \times \Delta\bar{H}_+^{(l)}$, as $\bar{E}^i$ is the known incident field and $\bar{E}_{int}^{(l-1)}$ and $\bar{H}_{int}^{(l-1)}$ are known from the solution of the $(l-1)$th iteration. It may be noted that (2) is equivalent to solving for the electric surface current density on the surface of a perfectly conducting object [24], [25] for a modified incident field as given by the left-hand side of (2). In particular, for the $l = 0$ iteration, the quantities $\bar{E}_{int}^{(-1)}$ and $\bar{H}_{int}^{(-1)}$ on the left-hand side of (2) are identically zero, so that the $l = 0$ iteration itself serves as the initial approximation on the external surface fields as required by IEBCM [19] provided that the object is assumed initially to be perfectly conducting. A step-by-step description of the lth iteration is now outlined as follows.

Step 1

a) The left-hand side of (2) is composed of two known quantities, the incident field $\bar{E}^i(\bar{r})$ and the integro-differential expressions involving the quantities $\bar{E}_{int}^{(l-1)}$ and $\bar{H}_{int}^{(l-1)}$ known from the previous iteration. Together these two quantities are expanded in terms of the vector spherical harmonics $\bar{M}_\nu^1(k\bar{r})$ and $\bar{N}_\nu^1(k\bar{r})$ with known expansion coefficients, i.e., [16]

$$\text{LHS (2)} = \sum_\nu D_\nu \left\{a_\nu \bar{M}_\nu^1(k\bar{r}) + b_\nu \bar{N}_\nu^1(k\bar{r})\right\} \quad (3)$$

where $\{a_\nu, b_\nu\}$ are the expansion coefficients, D_ν is a normalization term, while the composite index ν is actually a triple-index defined in [19]. It may be noted that for the $l = 0$ iteration (which also serves as the initial assumption), the fields $\bar{E}_{int}^{(-1)}$ and $\bar{H}_{int}^{(-1)}$ are identically zero so that $\{a_\nu, b_\nu\}$ are the coefficients for a vector spherical harmonic expansion of the known $\bar{E}^i(\bar{r})$ alone.

b) Likewise, the incremental external surface current $\hat{n} \times \Delta\bar{H}_+^{(l)}$ is expanded as follows [24], [25]:

$$\hat{n} \times \Delta\bar{H}_+^{(l)} = \sum_\nu \left\{ p_\nu \left[\hat{n} \times \bar{M}_\nu^1(k\bar{r})\right] + q_\nu \left[\hat{n} \times \bar{N}_\nu^1(k\bar{r})\right]\right\} \quad (4)$$

where $\{p_\nu, q_\nu\}$ are the unknown coefficients to be determined in this step.

c) Equations (3) and (4) are suitably truncated [25] and substituted in (2). Thereupon applying the orthogonality properties of the vector spherical harmonics, (2) is reduced to a system of simultaneous equations, which are then solved for the unknown coefficients $\{p_\nu, q_\nu\}$.

d) The external surface magnetic field $\bar{H}_+^{(l)}$ in the lth iteration is then calculated as the sum of the previously calculated value $\bar{H}_+^{(l-1)}$ and the incremental surface magnetic field $\Delta\bar{H}_+^{(l)}$ calculated for the lth iteration in c) above; i.e.,

$$\bar{H}_+^{(l)} = \bar{H}_+^{(l-1)} + \Delta\bar{H}_+^{(l)}. \tag{5}$$

It should be noted that although the solution procedure described in Step 1 is based on the regular EBCM, it could have, and it actually has been, alternatively solved using other methods such as the method of moments. Obviously there is no restriction on the specific method that can be used to obtain the initial assumption. We used the regular EBCM method to obtain the initial solution just for convenience since it is known that Waterman's solutions for *conducting* objects of aspect ratios as large as those of the models used in our calculations are still accurate [25]. This should not, however, be confused with the inadequacy of Waterman's method for *dielectric* objects of the same aspect ratios.

Step 2

a) The interior of the object is divided into a number of overlapping subregions $V^{(i)}$, as shown in Fig. 2 for the two geometries used in this paper. In each $V^{(i)}$, the internal fields $\{\bar{E}_{int,i}^{(l)}, \bar{H}_{int,i}^{(l)}\}$ are expanded in terms of a finite number of orthogonal functions, $\bar{\psi}_\nu(k'\bar{r})$, appropriate to the subregional geometry, with the unknown expansion coefficients to be determined; and $k' = k\sqrt{\epsilon_r^*}$.

b) To determine these unknown internal field expansion coefficients, the boundary condition

$$\hat{n}(\bar{r}) \times \bar{H}_+^{(l)}(\bar{r}) = \hat{n}(\bar{r}) \times \bar{H}_{int,i}^{(l)}(\bar{r}) \tag{6}$$

is satisfied on a suitable number of points on each of the subsurfaces $S^{(i)}$ and, in addition, the continuity of the internal magnetic field is enforced at a suitable number of points in each of the overlapping zones $OV^{(i,i+1)}$

$$\bar{H}_{int,i}^{(l)}(\bar{r}) = \bar{H}_{int,i+1}^{(l)}(\bar{r}) \tag{7}$$

where i and $i+1$ are two adjacent overlapping subregions.

c) Finally, the set of equations developed from (6) and (7) are simultaneously solved to determine the unknown coefficients of the multiple subregional internal field expansion. In this way the internal magnetic field $\bar{H}_{int}^{(l)}$, and the electric field $\bar{E}_{int}^{(l)}$, in the dielectric volume are determined in the lth iteration.

The iterative procedure as outlined in the Steps 1 and 2 above continues till the incremental electric surface current density $\hat{n} \times \Delta\bar{H}_+^{(l)}$ on the right-hand side of (2) becomes almost zero, thus meeting the preset error criterion.

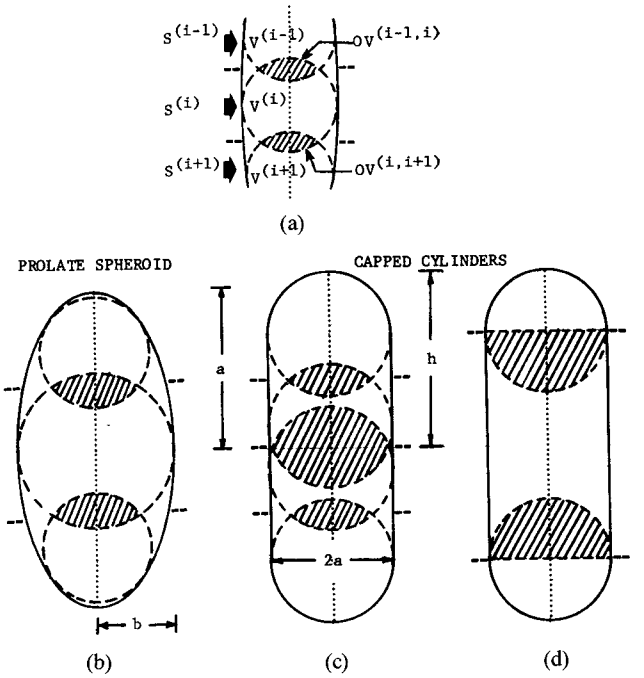

Fig. 2. Schematic illustrating the partitioning of the object volume V into subvolumes $V^{(i)}$ of convenient geometries. (a) The ith subregion has a subsurface $S^{(i)}$, and the shaded regions are the overlapping zones $OV^{(i,i+1)}$ [18], [19]. (b) Prolate spheroid subdivided into spherical subregions. Capped cylinder subdivided into (c) spherical subregions, and (d) into two spherical and one cylindrical subregions.

Once the internal field distribution has been obtained inside the model using the IEBCM, the absorbed power distribution is calculated as $1/2\sigma|\bar{E}_{int}(\bar{r})|^2$, where σ is the conductivity of the dielectric object. The average specific absorption rate (SAR), defined as the volume-normalized power deposition when the model is exposed to an incident power density of 10 W/m^2, is then obtained by averaging the absorbed power distribution over the entire model volume.

III. Description of the Computer Program

The IEBCM solution technique described above was implemented on the University of Utah UNIVAC 1161 computer. Specific cases of the incident plane-wave polarization, as well as specific object geometries, were considered in this program, and in this section we describe the salient features of the computer implementation of the IEBCM procedure.

The program was written in order to treat each m-order azimuthal mode separately since in the IEBCM, as well as in the EBCM [8], [25], it is possible to decouple the azimuthal modes when considering axisymmetric objects. The computer program has three chief subroutines, each of which shall now be discussed. In the MAIN routine the dielectric volume V is treated as a perfectly conducting object, and estimates of the surface electric current density $\hat{n} \times \bar{H}_+^{(l)}$ are obtained using the regular EBCM [25] in the lth iteration. Parenthetically, it should be noted that because of the smaller number of the coefficients required to

obtain a solution for the perfectly conducting objects, the regular EBCM solution procedure does not suffer from the ill-conditioning problems such as those encountered in the use of the EBCM for the case of lossy dielectric objects. The left-hand side of (2) is expanded in terms of the vector spherical harmonics, and known expansion coefficients $\{a_\nu, b_\nu\}$ are calculated for this expansion (3). A matrix defined in [25] is then calculated to relate the unknown coefficients $\{p_\nu, q_\nu\}$ of the incremental surface electric current density expansion $\hat{n} \times \Delta \bar{H}_+^{(l)}$, on the surface of the substitute perfectly conducting object, to the coefficients $\{a_\nu, b_\nu\}$. This matrix equation is then solved using the well-known LU decomposition scheme [26] to yield the coefficients of the expansion (4). This calculated increment $\hat{n} \times \Delta \bar{H}_+^{(l)}$ is then added to the value of $\hat{n} \times \bar{H}_+^{(l-1)}$ from the previous step, so that the output of the MAIN routine is a refined estimate $\hat{n} \times \bar{H}_+^{(l)}$ of the surface current density.

Once the estimate of $\hat{n} \times \bar{H}_+^{(l)}$ has been obtained for the particular azimuthal mode from the MAIN routine, then in the next subroutine STAGE2 a point-matching technique [27] is utilized to calculate the fields induced inside the actual dielectric object. As has been indicated previously, separate induced field expansions in terms of the basis functions $\bar{\psi}_\nu\ (k'\bar{r})$ are assumed in each subregion $V^{(i)}$. Collocation of the known $\hat{n} \times \bar{H}_+^{(l)}$ is carried out with the unknown $\hat{n} \times \bar{H}_{int,i}^{(l)}$ at suitable points on the corresponding subsurface $S^{(i)}$ to yield the system of (6); and the continuity of the internal fields is enforced by using the additional equations (7). In this way, by solving (6) and (7) simultaneously, the internal field expansions in all of the subregions $V^{(i)}$ are determined together.

Finally, with the knowledge of the estimates of the internal fields $\bar{E}_{int}^{(l)}$ and $\bar{H}_{int}^{(l)}$ in the lth step of the IEBCM, the program moves on into the last subroutine, called STAGE3. The quantity evaluated in this subroutine is

$$\nabla \times \int_S \left[\hat{n}(\bar{r}') \times \bar{E}_{int}^{(l)}(\bar{r}')\right] \cdot \bar{G}\,(k\bar{r}|k\bar{r}')\, ds'$$

$$-\nabla \times \nabla \times \int_S \frac{1}{j\omega\epsilon_0} \left[\hat{n}(\bar{r}') \times \bar{H}_{int}^{(l)}(\bar{r}')\right] \cdot \bar{G}\,(k\bar{r}|k\bar{r}')\, ds'$$

which is the term to be added to the incident field $\bar{E}^i(\bar{r})$ in the left-hand side of (2) for the $(l+1)$th iteration. In calculating this term, the integrations over the surface S are carried out using the Gauss-Legendre quadrature scheme [28].

IV. Numerical Results

As has been indicated above, we have chiefly utilized the IEBCM to study the power absorption characteristics of the axisymmetric, homogeneous, lossy dielectric models of biological objects irradiated by an incident plane wave at frequencies in and above the resonance frequency range. Average SAR values were calculated at different frequencies for the different models of an average man. Relevant information about the model dimensions, as well as about the relative complex permittivity of the model as a function of frequency, was obtained from [2].

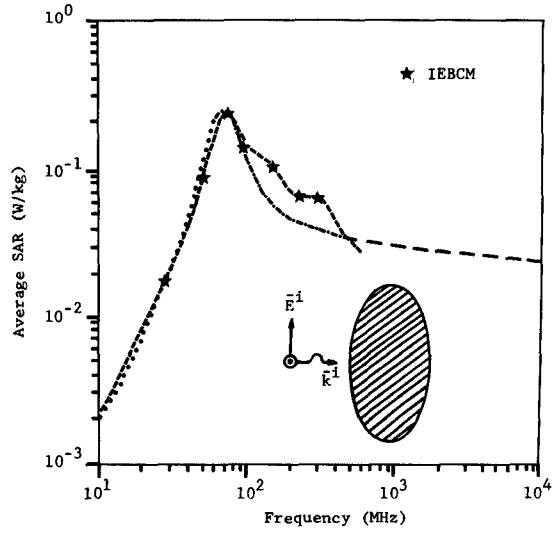

Fig. 3. Average SAR induced in a prolate spheroidal model of an average man ($a = 0.875$ m, $a/b = 6.34$) irradiated by an E-polarized plane wave. – – – is data from the block model of man [29], ····· from the prolate spheroidal model using EBCM [1, 2], –·–·– from an empirical formula [31], and —— from cylindrical models and geometrical optics [30]. The stars represent the calculated IEBCM results.

Studies conducted on the plane-wave exposure of the prolate spheroidal models have demonstrated that the maximum low-frequency absorption occurs when the incident electric field is oriented parallel to the major axis of the spheroid [1], [2]. This incident polarization, called the E-polarization, is, therefore, of great interest. For this polarization we tested the accuracy of the IEBCM solution technique as well as the continuity of the multiple subregional internal field expansion scheme, and the satisfactory results thus obtained have been reported in an earlier paper [19].

The calculated average SAR values obtained for the E-polarized plane-wave exposure of the man model are illustrated in Fig. 3, where they are compared with the results previously obtained using various computational and experimental approaches [1], [29]–[33]. It is clear from Fig. 3 that the IEBCM results agree very well with those obtained using the method of moments. Also, the IEBCM results for the spheroidal model showed fluctuations in the SAR values similar to those previously calculated using the block model of man [29]. Therefore, it is highly unlikely that these fluctuations are due to the part-body resonances, as indicated by others [29], [34], but instead they seem to be due to the higher order resonances. It should also be noted that the IEBCM made it possible to perform calculations up to 300-MHz frequency, which is about five times higher than that possible using the regular EBCM [1], [2].

For the E-polarized plane-wave exposure case we have discussed so far, the initial assumption on the external surface fields, as required by the IEBCM, was obtained, as indicated earlier, by replacing the lossy dielectric object by a perfectly conducting one of the same shape and size. Such a procedure, however, did not yield satisfactorily convergent internal field values even at 27 MHz for the case of the k-polarized plane-wave exposure of the man

model, i.e., when the incident wave propagation vector is aligned parallel to the major axis of the spheroid. The solution procedure for the k-polarization case was found to be particularly sensitive to the initial assumption, and hence we employed two other schemes to obtain convergent results. In the first scheme, we used another spheroidal model of the same shape and size but with the conductivity scaled up several times to be an intermediate step between the initial estimate and the biological model of interest. After obtaining a good convergent solution for this intermediate model, we used the solution thus obtained as an initial assumption for the biological model. More such intermediate steps were usually found necessary to finally get a convergent solution for the man model. This successive reduction of conductivity from a considerably larger value—usually between two to four times—to its actual value provided us with a good initial assumption for the problem involving the actual model conductivity, and we used this scheme for calculating stable and convergent internal field values up to 60 MHz for the man model.

The second scheme we employed involved the use of the internal fields calculated at a lower frequency to provide an initial assumption for the internal field calculation at the higher frequency of interest. For example, we used the internal fields calculated at 60 MHz to provide us with the starting solution at 120 MHz; and so on. This specifically allowed us to calculate results from 120 MHz to 300 MHz more economically than the first scheme mentioned above would have permitted us. This is because the number of iterations required for a convergent IEBCM solution was significantly reduced by the use of the second scheme.

An interesting consequence resulting from the utilization of this second scheme is that it may be possible to *hybridize the IEBCM with the available specialized low- and high-frequency techniques commonly used for solving EM boundary value problems* [35], [36]. Specifically, an "approximate" solution can be obtained either at a very low frequency or at a very high frequency using perturbational or asymptotic methods. This solution can, then, in turn, be used in the IEBCM solution procedure to calculate the correct fields at mid-range frequencies using the idea of a translation in frequency incorporated in the second scheme described above.

The calculated average SAR values for the k-polarized incident plane-wave exposure of the average man are illustrated in Fig. 4, where they are compared with the existing results obtained using the regular EBCM [1], [2] as well as from the surface integral equation (SIE) technique [37], [38] at higher frequencies. As is clear from Fig. 4, the correspondence between the IEBCM results and the existing average SAR values is satisfactory. In addition, as has already been pointed out, the use of IEBCM allows the calculation of stable internal field values at frequencies considerably higher than those permitted by the regular EBCM [2].

The various parameters in the computations of the E-polarized exposure case have already been presented in [19]. In most respects, the general computational considera-

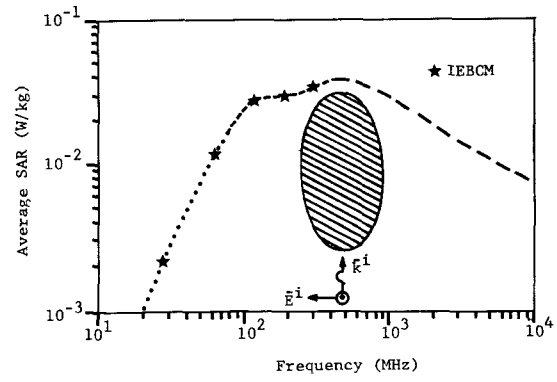

Fig. 4. Average SAR induced in a prolate spheroidal model of an average man ($a = 0.875$ m, $a/b = 6.34$) irradiated by a k-polarized plane wave. •••• is data from the same model using EBCM [1], [2], ---- from a capped cylindrical model using the SIE technique [38], and —— represent the estimated values [42]. The stars represent the calculated IEBCM results.

tions for the k-polarization case presented here are the same as for the E-polarized plane-wave incidence case. Due to the different methods of obtaining the initial assumption in the surface fields required for the k-polarization case, however, the number of iterations required for a convergent IEBCM solution is different from this exposure case. For the results shown in Fig. 4, three intermediate steps were required in the resonance frequency range. In the post-resonance range, however, results at a given frequency were computed using the computations made already at a lower frequency and so the IEBCM required a total of three to four iterations to converge. Although the model volume V was partitioned into nine overlapping spherical subregions at all the frequencies shown in Fig. 4, we feel, from the available results, that while only three subregions would have been adequate at 27 MHz, five would be required at 60 and 120 MHz, but nine would surely be needed at the higher frequencies. In addition, the number of the subregional field expansion coefficients varied from nine to twelve, the choice of the larger number being dependent on the electrical size and on the curvature of the particular subregion in a manner similar to that for the E-polarized plane-wave incidence case [19].

V. Extension of IEBCM to Composite Objects

The dielectric object considered so far is a prolate spheroid which is an example of a body whose surface can be defined by a single equation. A composite body, on the other hand, is constructed from several such simple bodies and thus has a surface defined by several equations in different sections of the total body. In order to investigate the applicability of the IEBCM solution procedure for composite bodies, we considered a lossy dielectric body made up of a finite cylinder with hemispherical end caps on either end, as shown in Fig. 2(c) and (d). It may be mentioned that such a body has a continuous normal everywhere on its surface.

The subregional geometry chosen for this body is immediately suggested by the object geometry itself. The capped cylinder was partitioned into a central finite cylin-

drical subregion with two spherical subregions on either end, as illustrated in Fig. 2(d). Spherical expansions [16] were used to represent the internal fields in the spherical subregions. The basis functions chosen for the cylindrical subregion will be considered in detail next.

The possible solutions of the scalar wave equation $(\nabla^2 + k'^2)\psi = 0$, regular at the origin, are given in a cylindrical coordinate system by [39]

$$\psi = J_m(\gamma_{nm}\rho)\, e^{\pm(j\beta_{nm}z)} e^{\pm(jm\phi)} \tag{8}$$

where $J_m(x)$ are the integral-order cylindrical Bessel functions, and

$$\gamma_{nm}^2 + \beta_{nm}^2 = k'^2. \tag{9}$$

Since we considered only the k-polarized plane-wave irradiation of this object, the azimuthal symmetries allowed us to consider the $m=1$ mode alone. Consequently, after dropping the index m in (8) and choosing the appropriate combinations of ψ, the following four solutions to the wave equation need alone be considered:

$$\psi_{\sigma n}^{\mathrm{TM}} = J_1\left(\gamma_{\sigma n}^{(\mathrm{TM})}\rho\right)\cos\phi \begin{Bmatrix} \cos\left(\beta_{\sigma n}^{(\mathrm{TM})}z\right) \\ \sin\left(\beta_{\sigma n}^{(\mathrm{TM})}z\right) \end{Bmatrix} \qquad \sigma = \begin{cases} \text{even} \\ \text{odd} \end{cases}$$

$$\psi_{\sigma n}^{\mathrm{TE}} = J_1\left(\gamma_{\sigma n}^{(\mathrm{TE})}\rho\right)\sin\phi \begin{Bmatrix} \cos\left(\beta_{\sigma n}^{(\mathrm{TE})}z\right) \\ \sin\left(\beta_{\sigma n}^{(\mathrm{TE})}z\right) \end{Bmatrix} \tag{10}$$

where the superscripts TM and TE denote the familiar transverse magnetic and electric modes, respectively, and σ can acquire two values—even or odd.

If now the vector potentials $\bar{A}$ and $\bar{F}$ are written as

$$\bar{A} = \hat{z}\psi^{\mathrm{TM}}, \quad \bar{F} = \hat{z}\psi^{\mathrm{TE}} \tag{11}$$

then the electric and the magnetic fields can be obtained thus

$$\bar{E} = -\nabla\times\bar{F} + j\omega\mu_0\bar{A} - \frac{1}{j\omega\epsilon_o\epsilon_r^*}\nabla(\nabla\cdot\bar{A}) \tag{12a}$$

$$\bar{H} = \nabla\times\bar{A} + j\omega\epsilon_o\epsilon_r^*\bar{F} - \frac{1}{j\omega\mu_0}\nabla(\nabla\cdot\bar{F}). \tag{12b}$$

It is well known that the various $\beta_{\sigma n}$'s used in (10) have a continuous spread of values from zero onward [23]. Computations involving a continuum of $\beta_{\sigma n}$ values would, however, be prohibitively impractical on a digital computer. We therefore chose discrete values of the $\beta_{\sigma n}$ in the following manner. If the cylindrical region of total height $2(h-a)$ in Fig. 2(d) is enclosed by two infinite perfectly conducting planes at $z = \pm d$, $d > h - a$, then the electric field components E_ρ and E_ϕ must be identically zero everywhere on these two conducting planes at $z = \pm d$. This permits us to select discrete values of the various $\beta_{\sigma n}$'s as

$$\beta_{on}^{(\mathrm{TM})}, \beta_{en}^{(\mathrm{TE})} = \frac{2n-1}{2}\frac{\pi}{d}, \qquad n = 1,2,\cdots$$

$$\beta_{en}^{(\mathrm{TM})} = n\frac{\pi}{d}, \qquad n = 0,1,2,\cdots$$

$$\beta_{on}^{(\mathrm{TE})} = n\frac{\pi}{d}, \qquad n = 1,2,\cdots. \tag{13}$$

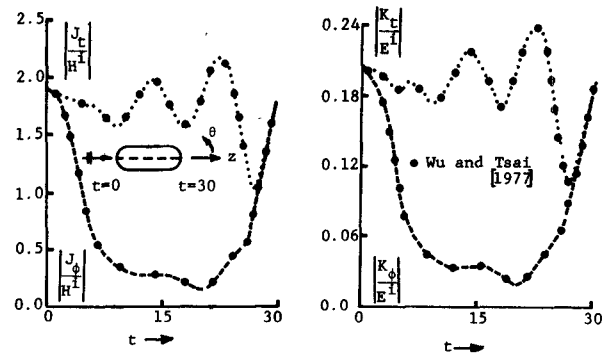

Fig. 5. Electric and magnetic surface current densities induced on a thick muscle capped cylinder ($h = 0.75\ \lambda$, $a = 0.2\ \lambda$, $\epsilon = 60\ \epsilon_0$, $\sigma = 1.0\ \Omega^{-1}m^{-1}$) irradiated by an incident k-polarized plane wave. $\bar{J} = J_t\cos\phi\hat{t} + J_\phi\sin\phi\hat{\phi}$, $\bar{K} = K_t\sin\phi\hat{t} + K_\phi\cos\phi\hat{\phi}$; where $\hat{t}$ and $\hat{\phi}$ are the unit transverse vectors in a $(\hat{n}, \hat{t}, \hat{\phi})$ coordinate system. The ordinate t is 0 at the lower end of the body and has a value of 30 at the upper end.

The choice of d itself in (13) is critical since in the real geometry of the problem the infinite conducting planes are nonexistent. In addition, $d > h - a$ since the true fields in the actual problem do not vanish at the ends of the cylindrical region or inside the body also. However, a suitable choice of d does provide us with a convenient discrete mode representation of the fields in the cylindrical region. We used several values of d in our calculations, and by checking on the convergence of the internal field distributions with respect to d, we were able to choose appropriate values of d.

Once the field representation inside the central cylindrical region was thus fixed, we tested the validity of the cylindrical expansion scheme as well as the applicability of the IEBCM to composite bodies by comparing the surface current densities obtained using the IEBCM calculations with those obtained for a similar object used by Wu and Tsai [40] using the SIE technique. The object chosen had a total height $2h = 1.5\lambda$ with a cross-sectional radius $a = 0.2\lambda$, and a permittivity of $60\epsilon_o$ with a conductivity of 1.0 $\Omega^{-1}\mathrm{m}^{-1}$.

The surface current densities, $\bar{J} = \hat{n}\times\bar{H}_+$ and $\bar{K} = \bar{E}_+\times\hat{n}$, obtained by the IEBCM calculations are compared with Wu and Tsai's computed values in Fig. 5. As is clear from this figure, the correspondence between the surface current densities obtained from the two solutions is very good, and thus validates both the use as well as the applicability of the IEBCM in solving for problems involving composite bodies. It may be mentioned here that d in (13) was chosen to be equal to $h + 18a$ for this calculation.

We finally address the issue of the choice of the basis functions used to represent the subregional internal fields induced inside the irradiated object. As has been indicated earlier, the IEBCM formulation is not restricted to the use of specific basis functions, and the choice of a particular set of basis functions should depend both on the subregional geometry as well as on the ease in generating these functions on a digital computer.

A convenient example was provided for this purpose by the case of the k-polarized plane-wave exposure of the composite capped cylinder discussed above. The interior

volume of the capped cylinder was first partitioned into spherical subregions as shown in Fig. 2(c) and the fields in each were expressed in terms of the spherical harmonics. Next, the same volume was divided into a central cylindrical subregion with two spherical subregions at both ends, as illustrated in Fig. 2(d). The cylindrical expansions described earlier were used to represent the fields in the cylindrical subregion, while the fields in the two spherical subregions were expressed in terms of the spherical harmonics.

On comparing the fields obtained inside such a capped cylindrical model of an average man ($h = 0.875$ m, $a = 0.1154$ m), at frequencies of 50 MHz and 300 MHz, we obtained good agreement in the results obtained using the two partitioning schemes. However, the reduction in the computational time when using the cylindrical expansions was considerable. By using nine spherical expansions to represent the internal fields, we utilized a total of 200 coefficients to determine the internal fields at both the frequencies considered, and the total CPU time expended per iteration ran into 200 s on the UNIVAC 1161 computer. On utilizing the cylindrical expansions in the central cylindrical subregion, on the other hand, the total number of the internal field coefficients was reduced to 88 at 50 MHz and to 104 at 300 MHz. This resulted in the CPU time expended to 77 s at 50 MHz and 114 s at 300 MHz on the same computer. This considerable reduction in computer time on using the interior partitioning scheme utilizing the cylindrical expansions is primarily due to the drastically reduced size of the point-matching matrix outlined in Step 2 of Section III. It should also be noted that the number of spherical expansions used in the partitioning scheme, which uses spherical subregions exclusively, did not lessen from nine at 50 MHz, the lower of the two frequencies considered. Schemes utilizing five and seven spherical expansions were experimented with at 50 MHz, but the smaller number of the spherical subregions thus used failed to represent the cylindrical volume adequately.

Since the total number of the IEBCM iterations required to obtain a convergent solution, however, did not change on using either of the subdivision schemes, we can conclude that it is more advantageous from the point of computational efficiency to choose convenient subregional geometries to represent the total model volume V. In addition, the basis functions used to represent the subregional fields should also be compatible with the subregional geometries used. It should be noted that although the iterative nature of the IEBCM facilitates the mechanical implementation of the solution procedure [20], [21], the *key* to the significant improvement of the regular EBCM *is* the use of the multiple subregional internal field expansion scheme [19], [41].

References

[1] P. W. Barber, "Scattering and absorption efficiencies for nonspherical dielectric objects—biological models," *IEEE Trans. Bio-Med. Eng.*, vol. BME-25, pp. 155–159, 1978.

[2] C. H. Durney, C. C. Johnson, P. W. Barber, H. Massoudi, M. F. Iskander, J. L. Lords, D. K. Ryser, S. J. Allen, and J. C. Mitchell, *Radiofrequency Radiation Dosimetry Handbook*, 2nd ed. Salt Lake City: University of Utah, 1978.

[3] M. F. Iskander, P. W. Barber, C. H. Durney, and H. Massoudi, "Near-field irradiation of prolate spheroidal models of humans," *IEEE Trans. Microwave Theory Tech.*, vol. MTT-28, pp. 801–807, 1980.

[4] A. Lakhtakia, M. F. Iskander, C. H. Durney, and H. Massoudi, "Irradiation of prolate spheroidal models of humans and animals in the near field of a small loop antenna," *Radio Sci.*, vol. 17(5S), pp. 77S–84S, 1982.

[5] A. Lakhtakia, M. F. Iskander, C. H. Durney, and H. Massoudi, "Near-field absorption in prolate spheroidal models of humans exposed to a small loop antenna of arbitrary orientation," *IEEE Trans. Microwave Theory Tech.*, vol. MTT-29, pp. 588–594, 1981.

[6] A. Lakhtakia, M. F. Iskander, C. H. Durney, and H. Massoudi, "Absorption characteristics of prolate spheroidal models exposed to the near fields of electrically small apertures," *IEEE Trans. Bio-Med. Eng.*, vol. BME-29, pp. 569–576, 1982.

[7] A. Lakhtakia and M. F. Iskander, "Scattering and absorption characteristics of lossy dielectric objects exposed to the near fields of aperture sources," *IEEE Trans. Antennas Propagat.*, vol. AP-31, pp. 111–120, 1983.

[8] P. C. Waterman, "Scattering by dielectric obstacles," *Alta Freq.*, vol. 38 (Speciale), pp. 348–352, 1969.

[9] P. C. Waterman, "Symmetry, unitarity, and geometry in electromagnetic scattering," *Phys. Rev. D*, vol. 3, pp. 825–839, 1971.

[10] P. C. Waterman, "Survey of T-matrix methods," in *Acoustic, Electromagnetic and Elastic Wave Scattering*, V. V. Varadan and V. K. Varadan, Eds. New York: Pergamon Press, 1980.

[11] R. H. T. Bates and D. J. N. Wall, "Null-field approach to scalar diffraction: I. General method; II. Approximate methods; III. Inverse methods," *Phil. Trans. Roy. Soc. London*, vol. A287, pp. 45–114, 1977.

[12] N. Morita, "Another method of extending the boundary condition for the problem of scattering by dielectric cylinders," *IEEE Trans. Antennas Propagat.*, vol. AP-27, pp. 97–99, 1979.

[13] G. Kristensson, "Electromagnetic scattering from buried inhomogeneities—A general three-dimensional formalism," *J. Appl. Phys.*, vol. 51, pp. 3486–3500, 1980.

[14] V. V. Varadan and V. K. Varadan, Eds., *Acoustic, Electromagnetic and Elastic Wave Scattering—Focus on T-Matrix Approach*. New York: Pergamon Press, 1980.

[15] B. Peterson and S. Strom, "T-matrix formulation of electromagnetic scattering from multilayered scatterers," *Phys. Rev. D*, vol. 10, pp. 2670–2684, 1974.

[16] J. A. Stratton, *Electromagnetic Theory*. New York: McGraw-Hill, 1941.

[17] D. J. N. Wall, "Methods of overcoming numerical instabilities associated with the T-matrix method," in *Acoustic, Electromagnetic and Elastic Wave Scattering*, V. V. Varadan and V. K. Varadan, Eds. New York: Pergamon Press, 1980.

[18] M. F. Iskander, A. Lakhtakia, and C. H. Durney, "A new iterative procedure to solve for scattering and absorption by lossy dielectric objects," *Proc. IEEE*, vol. 70, pp. 1361–1362, 1982.

[19] M. F. Iskander, A. Lakhtakia, and C. H. Durney, "A new procedure for improving the solution stability and extending the frequency range of the EBCM," *IEEE Trans. Antennas Propagat.*, vol. AP-31, pp. 317–324, 1983.

[20] R. Bansal, "A theoretical and experimental study of electromagnetic fields in finite dielectric cylinders," Ph.D. Thesis, Harvard Univ., Cambridge, MA, 1981.

[21] A. A. Sebak, L. Shafai, and A. Mohsen, "Generation of scattering data of imperfectly conducting objects from perfectly conducting ones," presented at the 1982 IEEE/AP-S Int. Symp., Albuquerque, NM, May 24–28, 1982.

[22] P. W. Barber and C. Yeh, "Scattering of electromagnetic waves by arbitrary shaped dielectric bodies," *Appl. Opt.*, vol. 14, pp. 2864–2872, 1975.

[23] P. M. Morse and H. Feshbach, *Methods of Theoretical Physics*. New York: McGraw-Hill, 1953.

[24] P. C. Waterman, "Matrix formulation of electromagnetic scattering," *Proc. IEEE*, vol. 53, pp. 805–812, 1965.

[25] P. C. Waterman and C. V. McCarthy, "Numerical solution of electromagnetic scattering problems," Mitre Corporation, Bedford, MA, Rep. MTP-74 (N69-31912), June 1968.

[26] G. Forsythe and C. B. Moler, *Computer Solution of Linear Algebraic Systems*. Englewood Cliffs NJ: Prentice-Hall, 1967.

[27] J. A. Morrison and M. J. Cross, "Scattering of a plane electromagnetic wave by axisymmetric raindrops," *Bell Syst. Tech. J.*, vol. 53, pp. 955–1019, 1974.
[28] M. Abramowitz and I. A. Stegun, *Handbook of Mathematical Functions*. New York: Dover, 1965.
[29] M. J. Hagmann, O. P. Gandhi, and C. H. Durney, "Numerical calculations of electromagnetic energy deposition in a realistic model of man," in *Abstracts Scientific Papers. URSI Int. Symp. Biological Effects Electromagnetic Waves*, Airlie, VA, Oct. 30–Nov. 4, 1977.
[30] H. Massoudi, C. H. Durney, and C. C. Johnson, "A geometrical-optics and an exact solution for internal fields in and energy absorption by a cylindrical model of man irradiated by an electromagnetic plane wave," *Radio Sci.*, vol. 14 (6S), pp. 35–42, 1979.
[31] C. H. Durney, M. F. Iskander, H. Massoudi, and C. C. Johnson, "An empirical formula for broadband SAR calculations of prolate spheroidal models for humans and animals," *IEEE Trans. Microwave Theory Tech.*, vol. MTT-27, pp. 758–763, 1979.
[32] O. P. Gandhi and M. J. Hagmann, "Some recent results on deposition of electromagnetic energy in animals and models of man," in *Abstracts Scientific Papers. URSI Int. Symp. Biological Effects Electromagnetic Waves*, Airlie, VA, Oct. 30–Nov. 4, 1977.
[33] M. F. Iskander, H. Massoudi, C. H. Durney, and S. J. Allen, "Measurements of the RF power absorption in spheroidal human and animal phantoms exposed to the near field of a dipole source," *IEEE Trans. Bio-Med. Eng.*, vol. BME-28, pp. 258–264, 1981.
[34] O. P. Gandhi, M. J. Hagmann, and J. A. D'Andrea, "Part-body and multibody effects on absorption of radio-frequency electromagnetic energy by animals and by models of man," *Radio Sci.*, vol. 14 (6S), pp. 15–21, 1979.
[35] J. Van Bladel, *Electromagnetic Fields*. New York: McGraw-Hill, 1964.
[36] R. Mittra, Ed., *Computer Techniques for Electromagnetics*. Oxford: Pergamon Press, 1973.
[37] T. K. Wu and L. L. Tsai, "Electromagnetic fields induced inside arbitrary cylinders of biological tissue," *IEEE Trans. Microwave Theory Tech.*, vol. MTT-25, pp. 61–65, 1977.
[38] H. Massoudi, C. H. Durney, P. W. Barber, and M. F. Iskander, "Postresonance electromagnetic absorption by man and animals," *Bioelectromagnetics*, vol. 3, pp. 333–339, 1982.
[39] R. F. Harrington, *Time-Harmonic Electromagnetic Fields*. New York: McGraw-Hill, 1961.
[40] T. K. Wu and L. L. Tsai, "Scattering from arbitrarily-shaped lossy dielectric bodies of revolution," *Radio Sci.*, vol. 12, pp. 709–718, 1977.
[41] A. Lakhtakia, "Near-field scattering and absorption by lossy dielectrics at resonance frequencies," Ph.D. thesis, Univ. of Utah, Salt Lake City, UT, 1983.
[42] C. H. Durney, M. F. Iskander, H. Massoudi, S. J. Allen, and J. C. Mitchell, *Radiofrequency Radiation Dosimetry Handbook*, 3rd ed. Salt Lake City: University of Utah, 1980.

✤

Akhlesh Lakhtakia (S'82) was born in Lucknow, India, on July 1, 1957. He received the B. Tech. degree in electronics engineering from the Banaras Hindu University, Varanasi, India, in June 1979. In September 1979 he entered the Graduate School, University of Utah, Salt Lake City, and obtained the M.S. degree in 1981 and the Ph.D. in 1983, both in electrical engineering.

From 1979 he has been employed as a Research Assistant in the Department of Electrical Engineering, University of Utah. He has been awarded a University of Utah Graduate Research Fellowship for the academic year 1982–1983. His research interests include the scattering and diffraction of electromagnetic waves, numerical electromagnetics, and microwave biological effects.

Dr. Lakhtakia is a member of the Electromagnetics Society.

Magdy F. Iskander (S'72–M'76) was born in Alexandria, Egypt, on August 6, 1946. He received the B.Sc. degree in electrical engineering, University of Alexandria, Egypt, in 1969. He entered the Faculty of Graduate Studies at the University of Manitoba, Winnipeg, Man., Canada, in September 1971, and received the M.Sc. and Ph.D. degrees in 1972 and 1976, respectively, both in microwaves.

In 1976 he was awarded a National Research Council of Canada Postdoctoral Fellowship at the University of Manitoba. Since March 1977 he has been with the Department of Electrical Engineering and the Department of Bioengineering at the University of Utah, Salt Lake City, UT, where he is currently an Associate Professor of Electrical Engineering. In 1981 he received the University of Utah President David P. Gardner Faculty Fellow award and spent the academic quarter on leave as a Visiting Associate Professor at the Department of Electrical Engineering and Computer Science, Polytechnic Institute of New York, Brooklyn, NY.

Dr. Iskander edited a special issue of the *Journal of Microwave Power* on "Electromagnetics and Energy Applications," in March 1983, and is presently editing another special issue of the same journal on "Electromagnetic Techniques in Medical Diagnosis and Imaging." His present fields of interest include the scattering and diffraction of electromagnetic waves, antenna design, and the biological effects as well as the medical applications of electromagnetic waves.

✤

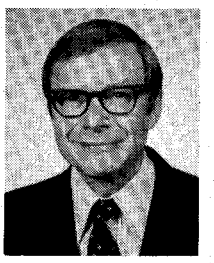

Carl H. Durney (S'60–M'64–SM'80) was born in Blackfoot, ID, on April 22, 1931. He received the B.S. degree in electrical engineering from Utah State University, Logan, in 1958, and the M.S. and Ph.D. degrees in electrical engineering from the University of Utah, Salt Lake City, in 1961 and 1964, respectively.

From 1958 to 1959 he was employed as an Associate Research Engineer with the Boeing Airplane Company, Seattle, WA, where he studied the use of delay lines in control systems. He has been with the University of Utah since 1963, when he was appointed to be Assistant Research Professor of Electrical Engineering. From 1965 to 1966 he was employed at the Bell Telephone Laboratories, Holmdel, NJ, while on leave from the University of Utah. During this time, he worked in the area of microwave avalanche diode oscillators.

Again, in 1971, he was engaged in study and research involving microwave biological effects at the University of Washington while on leave from the University of Utah. From 1977 to 1982 he was chairman of the Electrical Engineering Department at the University of Utah, where he is presently Professor of Electrical Engineering and engaged in teaching and research in electromagnetics, engineering pedagogy, and microwave biological effects.

Dr. Durney is a member of The Bioelectromagnetics Society, Commission B of URSI (International Union of Radio Science), Sigma Tau, Phi Kappa Phi, Sigma Pi Sigma, Eta Kappa Nu, and the American Society for Engineering Education. He also served as Vice President (1980–1981) and President (1981–1982) of The Bioelectromagnetics Society, as a member (1979–present) and Chairman (1983–present) of the IEEE Committee on Man and Radiation (COMAR), as a member of the American National Standards Institute C95 Subcommittee IV on Radiation Levels and/or Tolerances with Respect to Personnel (1973–present), as a member of the editorial board of the IEEE TRANSACTIONS ON MICROWAVE THEORY AND TECHNIQUES (1977–present), and as a member of the editorial board of *Magnetic Resonance Imaging* (1982–present). In 1980 he received the Distinguished Research Award from the University of Utah, and the Outstanding Teaching Award, College of Engineering, University of Utah. In 1982, he received the American Society for Engineering Education Western Electric Fund Award for excellence in teaching, and the Utah Section IEEE Technical Achievement Award. He was named a College of Engineering Distinguished Alumnus by Utah State University in 1983.